641. Multiphysical modeling of a contact-type piezo-transducer for the analysis of micro-energy harvesting from ambient vibrations

R. Daukševičius[1,2,a], G. Kulvietis[1,b], V. Ostaševičius[2,c], R. Gaidys[2,d], I. Milašauskaitė[2,e]
[1] Vilnius Gediminas Technical University, Saulėtekio al. 11, LT-10223 Vilnius, Lithuania
[2] Kaunas University of Technology, Studentų 65, LT-51369 Kaunas, Lithuania
E-mail: [a] *rolanasd@centras.lt,* [b] *genadijus_kulvietis@gama.vtu.lt,* [c] *vytautas.ostasevicius@ktu.lt,* [d] *rimvydas.gaidys@ktu.lt,* [e] *ieva.milasauskaite@gmail.com*

(Received 10 January 2011; accepted 28 March 2011)

Abstract. The paper presents development of a coupled-field finite element model of a contact-type piezoelectric transducer, which acts as a micropower source for MEMS sensors by harvesting energy from ambient vibrations. The proposed FE model of the cantilever-type piezotransducer couples three different physical domains: mechanical, piezoelectrical and fluidic. Both linear and nonlinear piezoelectric models are implemented. The fluid-structure interaction is modeled as viscous air damping, which manifests in the form of squeeze-film damping governed by the nonlinear compressible isothermal Reynolds equation. Vibro-impact interaction is modeled through implementation of a special adhesive-repulsive contact model that is suitable for contact simulations at the micro-scale. Performance of the FE model is demonstrated by representative dynamic simulations including parametric studies that reveal the influence of structural, excitation and ambient pressure parameters on dynamical and electrical performance of the device.

Keywords: energy harvesting, piezoelectric micropower generator, coupled-field, finite element modeling, nonlinear squeeze-film damping, contact, vibro-impact interaction, dynamics.

1. Introduction

Continuous improvements in energy efficiency of low-power integrated circuits and rapid progress of microfabrication technologies have enabled realization of a large variety of battery-powered devices such as wireless sensors, implantable medical microsystems and various portable devices. However, there is a strong need to reduce or even eliminate the dependency on battery power since maintenance, replacement and disposal of batteries is costly, time consuming and environmentally hazardous. This is particularly true in the case of large autonomous wireless sensor networks with their potential diverse applications in the fields of condition monitoring and ambient intelligence within industrial, civilian, healthcare, environmental, security and other sectors. Furthermore, battery powering is highly undesirable or entirely unacceptable in the case of implanted medical devices or sensors embedded permanently inside the structures such as buildings, roads, railways, bridges, dams, airframes and various long-term installations operating in remote harsh environments including boreholes and other subsurface structures as well as nuclear reactors, oil-gas reservoirs, deep-sea or space infrastructures. Therefore, **energy harvesting** concept is actively developed as an alternative solution that will provide either primary or supplementary power depending on the application. Different harvesting approaches are considered including thermoelectric and photovoltaic effects, RF power conversion and harnessing of mechanical motion. The latter is particularly

attractive since: a) potential power density levels are fairly attractive, b) structural vibrations are encountered around most machines, structures or biological systems. Kinetic energy harvesting is considered to be a highly promising solution for powering autonomous sensors for **in situ** structural health monitoring of various structures. Electromagnetic, electrostatic and piezoelectric transduction principles are used to convert vibrations into electrical energy. Piezoelectric conversion has an advantage of higher energy density with respect to the other two transduction methods. Piezoelectric micropower generators (PMPGs) also benefit from relatively simple geometry, fewer peripheral components and relative ease of fabrication [1-4].

Majority of vibrational PMPGs are spring-mass-damper systems (in cantilever configuration), which deliver maximum power when input vibration matches their resonant frequency. This means that these generators have a very narrow operating frequency range (bandwidth). The main complication in this case is that prevalent environmental vibrations are of random nature, varying widely in frequency and amplitude. Common sources, such as household appliances and manufacturing equipment generate vibrations with amplitudes of 0.2 – 10 m/s^2 at frequencies of 60 – 200 Hz. However, in the case of most production machinery, usual vibration levels may be very low (< 1 m/s^2) at frequencies corresponding to that of the mains (i.e. 50/60 Hz or harmonics). This fact severely restricts power-generation capability and practical usability of resonant-type PMPGs for powering of most electronics including MEMS-based sensors [2-5].

From the structural point of view there may be distinguished two principal groups of design approaches that are used to maximize energy collection in these generators: a) improvement of piezoelectric "domain" (optimization of geometry, electrode configuration, material properties), maximization of proof mass in order to increase input kinetic energy and minimization of the dissipation in the vibrating piezoelectric transducer; b) expansion of operating frequency range of the PMPG by tuning its resonant frequency or widening the bandwidth [2-5].

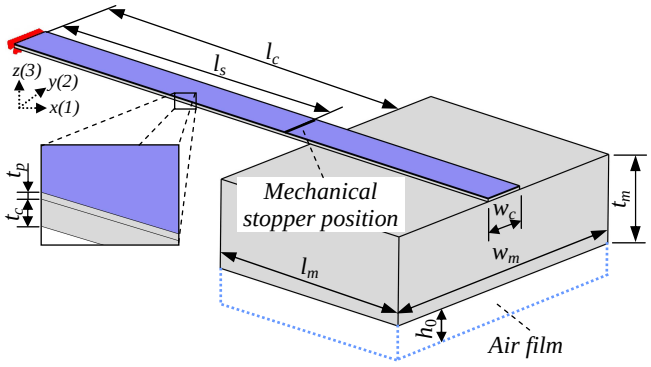

Fig. 1. Scheme of the developed finite element model of a cantilever-type double-layer piezotransducer with proof mass at the free end. Zoomed area shows double-layer structure of the cantilever consisting of the supporting Si layer t_c and the piezoelectric layer t_p atop. Air film of thickness h_0 is present between an imaginary fixed ground surface and the bottom face of the proof mass (drawn not to scale). It is considered that mechanical stopper is placed underneath the piezotransducer at vertical distance h_s from the bottom face and horizontal distance l_s from the cantilever anchor

2. Multiphysical modeling of the piezotransducer

Accurate simulation models are required in order to enable development of effective and efficient vibrational PMPGs. Therefore present study is devoted to finite element modeling of the cantilever-type piezotransducer, which represents a common structure used in the majority of PMPGs. Two types of cantilever configurations are considered: basic single-layer

piezoelectric cantilever structure and double-layer cantilever, which has the proof mass attached at the free end and consists from the piezoelectric layer and the supporting layer (the shim) (Fig. 1 and Table 1). The developed FE model will serve for the numerical studies of the aforementioned design approaches used for enhancement of harvesting efficiency including influence of proof mass, configuration of the piezoelectric "domain", dissipation due to microscale-dominant viscous air damping and PMPG bandwidth widening by implementing vibro-impact interaction using a mechanical stopper. The complexity of FE modeling and simulation of the piezotransducer is associated with the *coupled-field* (*multiphysical*) nature of the device, where different energy domains (mechanic, piezoelectric, fluidic) interact with each other and, therefore, independent solution of one domain is generally impossible without simultaneous solution of the others. The time-dependent solution of this numerical problem is further complicated by nonlinear character of the considered physical phenomena, particularly in the case of vibro-impact and fluidic-structural interactions (meanwhile linear piezoelectricity may be applied in some simulation cases).

Table 1. Geometric parameters of the modeled piezotransducers

Parameter	**Double-layer piezotransducer with proof mass**	**Single-layer piezotransducer without proof mass**
	Value, μm	
Length of uniform cantilever l_c	2500	3000
Length of proof mass l_m	1500	-
Width of cantilever w_c	300	150
Width of proof mass w_m	3000	-
Thickness of cantilever supporting layer t_c	20	-
Thickness of piezoelectric layer t_p	20	20
Thickness of proof mass t_m	1000	-

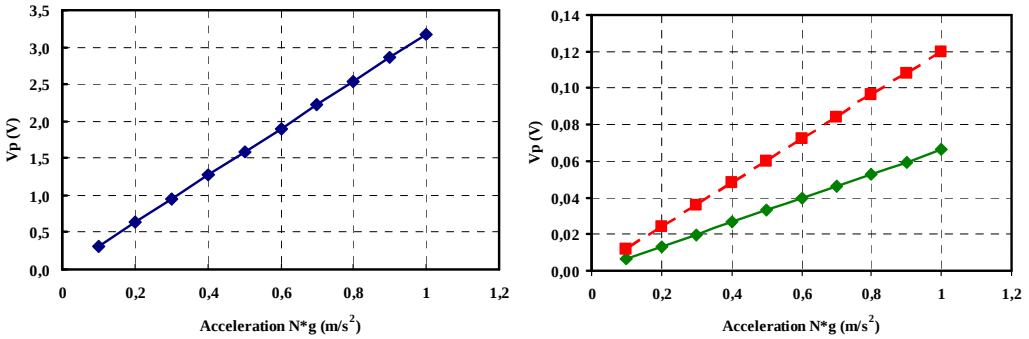

(a) (b)

Fig. 2. Peak voltage as a function of applied acceleration a=Ng during harmonic base excitation of the double-layer piezotransducer with the proof mass at: (a) fundamental frequency, (b) 60 Hz (solid green line), (b) 120 Hz (dashed red line)

The modeled piezotransducer illustrated in Fig. 1 consists of the supporting cantilever layer made from silicon and the top layer of piezoceramics PZT-5A, which is chosen arbitrarily as a typical representative of this class of materials (application of the piezoelectric polymer PVDF is considered by the authors as an attractive candidate for energy harvesting applications [6]). It is poled along the thickness (*z(3)* axis) direction resulting in a transverse ("d_{31}") operation

mode. Cantilever configuration is chosen since: a) for the given loading it produces the highest average strain, which directly determines the power output; b) cantilever-type fixing condition results in the lowest resonant frequency for a given device size. In addition, large proof mass is mounted at the free end of the piezotransducer in order to further reduce its resonant frequency and to increase the produced strain enabling to achieve higher power output.

Finite element models of the piezotransducer were realized in the "Piezoelectric Application" mode of the COMSOL Multiphysics, which uses constitutive equations of either linear or nonlinear piezoelectricity (see Chapter 2.1). Piezoelectric layer has got electrodes on its bottom and top faces, which are perpendicular to *z(3)* axis. Due to low thickness the mechanical behavior of the electrodes is neglected. Their electrical behavior is evaluated by imposing proper electrostatic boundary conditions: the bottom face is grounded, while the top one is set to "Floating potential" condition. For the rest of faces of the piezoelectric layer the condition of "Zero charge/Symmetry" is applied. Input vibrations are assumed to be acting along *z(3)* axis. These vibrations are represented as sinusoidal kinematic excitation by applying vertical acceleration through body load equal to $F_z = a\rho$, where a = Ng (N - multiplier, g = 9.81 m/s^2) and ρ is density of the corresponding material (Si or PZT-5A).

2.1 Piezoelectrical modeling

During contact-type operation of the piezotransducer higher vibration modes may be excited including both flexural and torsional modes. Large proof mass mounted at the end of the cantilever increases the deformation of the cantilever. The aforementioned conditions may induce large displacements or rotations of the piezotransducer resulting in geometric nonlinearities. Therefore large-deformation (nonlinear) piezoelectrical equations are used for the FE model of the piezotransducer [7,8]. The resulting strains are calculated using the following Green-Lagrange strain-displacement relation:

$$\varepsilon_{ij} = \frac{1}{2}\left(\frac{\partial u_i}{\partial x_j} + \frac{\partial u_j}{\partial x_i} + \frac{\partial u_k}{\partial x_i}\cdot\frac{\partial u_k}{\partial x_j}\right). \quad (1)$$

The main constitutive equations for the large deformation piezoelectricity are:

$$S = c_E\varepsilon - e^T\mathbf{E}_m, \quad (2)$$

$$\mathbf{P}_m = e\varepsilon + \left(\varepsilon_0\varepsilon_{rS} - \varepsilon_0\mathbf{I}\right)\mathbf{E}_m. \quad (3)$$

where S is the second Piola-Kirchhoff stress, ε is the Green strain, $\mathbf{E}_m$ and $\mathbf{P}_m$ are the matrices for electric field and polarization in the material orientation, $\mathbf{I}$ is identity matrix, c_E, e, ε_{rS} are constants of a piezoelectric material, ε_0, ε_r – vacuum and the relative permittivity respectively.

Eqs. (2)-(3) mean that: a) electrical field variables are calculated in the material directions, and the electric displacement relation is replaced by an expression that produces electric polarization in the material orientation of the solid; b) the electrical energy is split into two parts: the polarization energy within the solid and the electric energy of free space occupied by the deformed solid.

The relationship for electric displacement field in the material orientation is represented as:

$$\mathbf{D}_m = \mathbf{P}_m + \varepsilon_0 JC^{-1}\mathbf{E}_m, \quad (4)$$

$$C = F^T F, \quad (5)$$

$$F = \frac{\partial \mathbf{x}}{\partial \mathbf{X}}. \quad (6)$$

where C is the right Cauchy-Green tensor, F is the deformation gradient, which is defined as the gradient of the present position of a material point $\mathbf{x} = \mathbf{X} + \mathbf{u}$, J is the determinant of F.

The following transformations are applied to obtain the fields in the global orientation:

$$\mathbf{E} = F^{-T}\mathbf{E}_m, \quad \mathbf{P} = J^{-1}F\mathbf{P}_m, \quad \mathbf{D} = J^{-1}F\mathbf{D}_m, \quad \rho_q = \rho_{q_m}J^{-1}. \tag{7}$$

where ρ_q, ρ_{q_m} are the volume charge density in present and material coordinates.

In the case when the piezotransducer undergoes relatively small deformations (e.g. operation without impacting involved) the piezoelectrical model may be simplified by using the constitutive relations of the linear piezoelectricity [9]:

$$\begin{aligned} \sigma &= c_E\varepsilon + e^T\mathbf{E}, \\ \mathbf{D} &= e\varepsilon + \varepsilon_0\varepsilon_{rS}\mathbf{E}. \end{aligned} \tag{8}$$

where σ is the stress vector, ε is the strain vector, e is the matrix of piezoelectric stresses, $\mathbf{D}$ is the electric charge density vector, $\mathbf{E}$ is the electric field intensity vector.

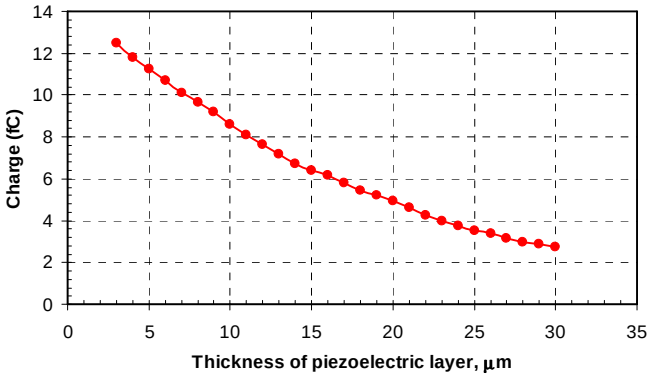

Fig. 3. Variation of generated charge as a function of the piezoelectric layer thickness t_p

FE model of the double-layer piezotransducer with the proof mass (based on linear piezoelectric model) was used to perform a series of parametric simulations, which provided the dependencies demonstrating the influence of geometrical and input vibration parameters on generated charge and voltage. These results, which are presented in detail in [8], are indispensable for the design of the efficient PMPG. Figs. 2-3 are included in this paper to show some of the representative results of the analysis.

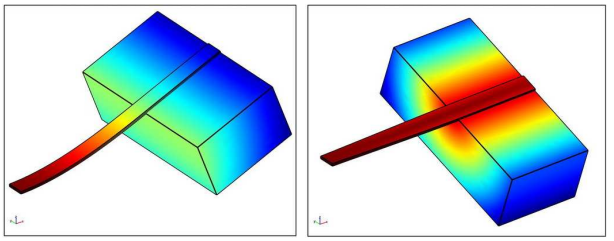

(a) (b)

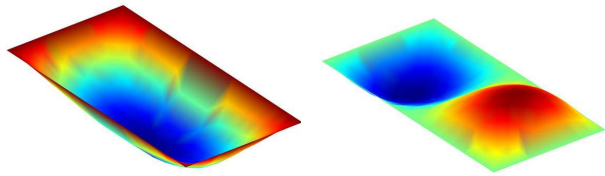

(c) (d)

Fig. 4. The first two vibration modes of the analyzed PMPG: (a) the 1st out-of-plane flexural mode (184 Hz), (b) the 1st torsional mode (458 Hz). (c)-(d) 3D contour plots illustrating the distribution of air pressure forces in the gap for the corresponding structural mode shapes

2.2 Modeling of nonlinear viscous air damping

If the micro-scaled piezotransducer is designed to operate in ambient pressure, the air may strongly influence dynamic performance of the PMPG due to the effect of so-called squeeze-film damping, a type of viscous air damping, which is the predominant source of energy loss in MEMS devices [10]. It manifests when a microstructure of relatively large lateral dimensions (with respect to air gap size) moves towards/outwards in relation to a fixed surface with a thin air-film in between. Such situation is particularly plausible in the case of a piezotransducer with a bulky proof mass at the end of the cantilever structure: if the bottom face of the proof mass is located relatively close to some stationary ground surface (e.g. substrate), then during transverse motion of the mass its fairly small displacement in normal direction would squeeze out the air from the narrow gap. However, air viscosity will limit the flow rate along the gap, and thus the pressure will be increased inside the gap resulting in a counter-reactive force that will oppose the motion of the vibrating cantilever structure. On the continuous field level, squeeze-film damping of a microstructure vibrating in a fluid is governed by the Navier-Stokes (NS) equations. Their solution by means of CFD techniques is extremely expensive from the computational point of view and in the case of multiphysical 3D systems (as in the PMPG) such approach is hardly feasible with stand-alone computers. Reynolds equation, known from lubrication theory, could be adapted for modeling of the squeeze-film damping in the piezotransducer [10]:

$$\frac{\partial}{\partial x}\left(\frac{\rho h^3}{\mu}\frac{\partial P}{\partial x}\right)+\frac{\partial}{\partial y}\left(\frac{\rho h^3}{\mu}\frac{\partial P}{\partial y}\right)=6\left\{2\frac{\partial(\rho h)}{\partial t}+\frac{\partial}{\partial x}\left[\rho h(u_1+u_2)\right]+\frac{\partial}{\partial y}\left[\rho h(v_1+v_2)\right]\right\}. \quad (9)$$

where fluid density ρ, pressure in the gap P, and the gap thickness h are functions of time and position (x, y). μ is the dynamic viscosity of the fluid, u_1 and u_2 are the velocities in the x-direction of the top and the bottom surface, respectively, and v_1 and v_2 are the velocities in the y-direction of the two surfaces.

Reynolds equation is a nonlinear partial differential equation, which is derived from NS equation, the equation for the conservation of mass and the equation of state for an ideal gas by assuming that: a) the fluid is treated as continuum and is Newtonian, does not slip at the boundaries and obeys the ideal gas law; b) the inertia and body forces are negligible compared to the viscous and pressure forces; c) pressure variation across the fluid film is negligible; d) the flow is laminar; e) the thickness of fluid film is very small compared to the lateral dimensions of structures.

Since the relative movement in lateral direction does not occur in the piezotransducer, the original Reynolds equation is reduced to:

$$\frac{\partial}{\partial x}\left(\frac{\rho h^3}{\mu}\frac{\partial P}{\partial x}\right)+\frac{\partial}{\partial y}\left(\frac{\rho h^3}{\mu}\frac{\partial P}{\partial y}\right)=12\frac{\partial(\rho h)}{\partial t}. \tag{10}$$

Gas is a predominant working fluid in MEMS devices and thin gas films are realistically assumed to be isothermal. For isothermal process P/ρ is constant and therefore density in the Reynolds equation can be replaced with pressure, thereby yielding the isothermal compressible Reynolds equation that is used to evaluate the magnitude of squeeze-film damping in the piezotransducer:

$$\frac{\partial}{\partial x}\left(h^3 P\frac{\partial P}{\partial x}\right)+\frac{\partial}{\partial y}\left(h^3 P\frac{\partial P}{\partial y}\right)=12\mu_{eff}\left(h\frac{\partial P}{\partial t}+P\frac{\partial h}{\partial t}\right), \tag{11}$$

$$\mu_{eff}=\frac{\mu}{1+9.638\left(\frac{L_0 P_a}{p_0 h_0}\right)^{1.159}}. \tag{12}$$

where μ_{eff} is the effective viscosity coefficient, which is used to account for gas rarefaction effects (a model of T. Veijola [11] is used here; it is adopted by the COMSOL Multiphysics as one of the optional approaches), p_0 is the initial (ambient) pressure in the gap, L_0 is the mean free path of air particles at atmospheric pressure P_a, and h_0 is the initial air-film thickness. For the P_a = 101325 Pa, $L_0 \approx$ 65 nm. Total pressure in the gap is equal to $P = p_0 + \Delta p$, where Δp is an additional air pressure variation due to the squeezed air-film effect.

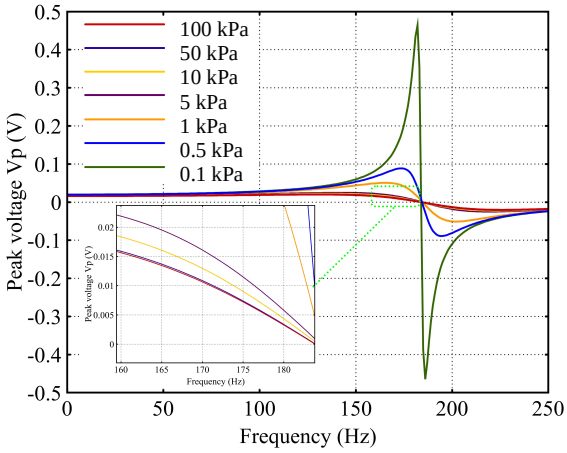

Fig. 5. Voltage responses obtained in the vicinity of the fundamental frequency of the PMPG in the presence of squeeze-film damping for a constant air-film thickness (h_0 = 50 μm) at different levels of ambient pressure p_0: 100 Pa, 500 Pa, 1 kPa, 5 kPa, 10 kPa, 50 kPa, 100 kPa (a = 0.1g)

"Film Damping Application" mode of the COMSOL, that makes use of eqs. (11) and (12), was added to the piezoelectrical model of the PMPG, which enables running dynamic simulations of the device taking into account the effect of squeeze-film damping. Numerical modal analysis was carried out in order to check the effectiveness of the multiphysics FE model. Fig. 4 illustrates the obtained structural and pressure mode shapes, which reveal the distribution of air pressure forces in the gap when the structure is vibrating in its flexural and

torsional resonant modes. The coupling between structural displacements and the resulting pressure forces is obvious: the upward motion of the right side of the proof mass in Fig. 4(b) corresponds to a convex profile in a respective region of the pressure mode shape (Fig. 4(d)), which demonstrates the compression effect, i.e. pressure increase in the gap with respect to the atmospheric.

Frequency response analysis was carried out in order to determine influence of air damping on voltage output of the PMPG. Zero structural damping was used for these simulations. Parametric solver was applied in order to sweep over the frequency range of 0 – 250 Hz. Thereby a series of voltage responses were computed with different values of initial ambient pressure p_0 (Fig. 5). The variation of peak voltage with frequency indicates that in the considered case (h_0 = 50 μm), ambient pressures of more than 1 kPa severely damps the motion of the piezotransducer, which results in a considerable drop in the voltage output. The magnified portions of voltage curves in the inset of Fig. 5 reveal that the magnitude of induced squeeze-film damping is very similar for ambient pressures that are in the range of 10 – 100 kPa.

2.3 Formulation of the contact model

Contact-mode operation of the piezotransducer is one of the possible approaches for expanding operating frequency range of the PMPG. This approach allows realization of frequency up-conversion mechanism since the strongly nonlinear character of the vibro-impact interaction due to cantilever impacting against the mechanical stopper (amplitude limiter) can be used to stabilize the generated voltage in the case of varying frequency of input vibrations [5].

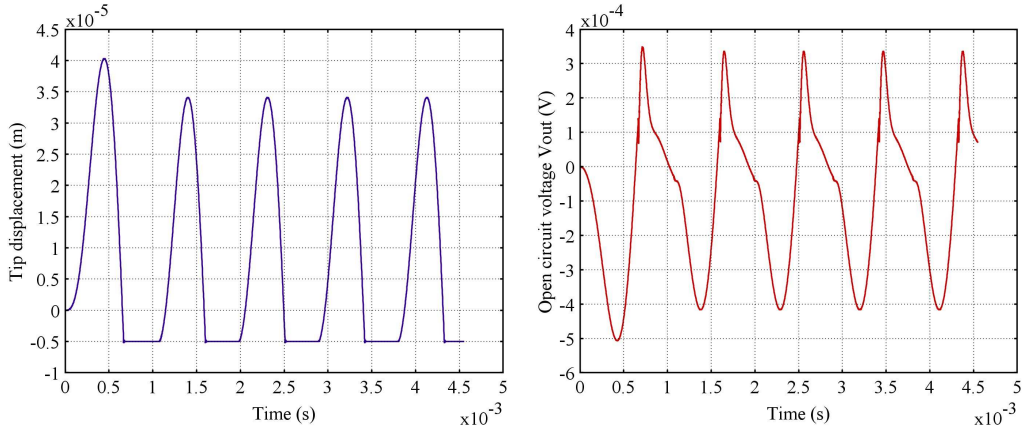

(a) (b)

Fig. 6. (a) Transient impacting motion of the single-layer piezotransducer with mechanical stopper during harmonic base excitation at the fundamental frequency (h_s = 5 μm, k_p = 10^8, l_s/ l_c = 1), (b) the corresponding temporal variation of the open circuit voltage

At this stage the contact model was implemented into the FE model of the single-layer piezotransducer without the proof mass because it is prudent to check model performance by using a more simple geometrical structure in order to maintain solution times of nonlinear transient problems within reasonable limits. It should be noted that even the current model of uniform single-layer piezoelectric cantilever is a challenge for COMSOL numerical solvers

since all the evaluated physical phenomena (piezoelectricity, squeeze-film damping, vibro-impact interaction) are nonlinear. The model of the double-layer piezotransducer with the proof mass significantly increases the number of degrees of freedom therefore the required computational effort becomes easily prohibitive in the case of dynamic simulations with contact.

When formulating contact model it is considered that the mechanical stopper is placed underneath the piezotransducer at vertical distance h_s from the bottom face and horizontal distance l_s from the cantilever anchor. The impact is modeled on the basis of contact element approach, which means that impact forces generated during collision of the piezotransducer and the stopper are represented by a linear elastic element, which is activated when the structures come into contact. The element is characterized by "penalty" stiffness coefficient k_p. In addition, the proposed model may be adapted to the case of micro-scale contacts, where it is necessary to take into account the contribution of adhesion, which is evaluated here by the attractive van der Waals force component. The obtained attractive-repulsive contact model is represented by a shear force $F_s(t)$ that is applied along the width (edge) of the piezotransducer:

$$F_s(t)=\begin{cases}\dfrac{C_{vdW}}{\left[h_s-z_{l_s}(t)\right]^3} & for\ z_{l_s}(t)<h_s-\xi_0,\\ \dfrac{C_{vdW}}{\xi_0^3}-k_p\left[z_{l_s}(t)-\left(h_s-\xi_0\right)\right] & for\ z_{l_s}(t)\geq h_s-\xi_0.\end{cases} \tag{13}$$

where h_s - gap between the piezotransducer and the stopper, ξ_0 - interatomic distance at equilibrium at the interface between the piezotransducer and the gap; $z_{ls}(t)$ - displacement of the piezotransducer. The interaction is modeled: a) before contact ($z_{ls}(t) < h_s - \xi_0$) - by attractive van der Waals force component that is proportional to constant parameter $C_{vdW} = A_h A_c/6\pi$ and decays with the third power of the separation distance (A_h - Hamaker constant, A_c - contact area), b) upon contact ($z_{ls}(t) \geq h_s - \xi_0$) - by repulsive elastic force that is proportional to "penalty" stiffness coefficient k_p and grows linearly with the penetration distance.

Due to the size of the modeled piezotransducer the contribution of adhesion may be neglected ($C_{vdW} = 0$). Impact simulations revealed that the best numerical convergence is achieved for the "penalty" coefficient $k_p = 10^7 \div 10^8$.

Fig. 6 illustrates the results of the preliminary transient simulations that demonstrate the vibro-impact motion of the single-layer piezotransducer (based on the nonlinear piezoelectric model) and the corresponding variation of the open circuit voltage. In the future the FE model will be fine-tuned in order to ensure better convergence and faster computations.

Conclusions

The paper described a multidisciplinary finite element model of the contact-type piezotransducer, which evaluates all of the major physical interactions that are active during device operation. The simulated effects include (non)linear piezoelectricity, nonlinear squeeze-film damping as well as nonlinear vibro-impact interaction. The proposed FE model is flexible and versatile: a) it can be adjusted to different device configurations (structural boundary conditions, inclusion/exclusion of proof mass, various PZT electrode arrangements, etc.); b) piezoelectric and air damping phenomena may be simulated either using nonlinear governing equations or using their linear or linearized formulations when the type of dynamic analysis justifies such simplification (e.g. during frequency response analysis); c) the proposed contact model is adaptive - it allows to specify various interaction states, which may range from fully-repulsive (i.e. intermolecular interactions are neglected) to a mixed adhesive-repulsive conditions that may occur in the case of micro-scaled contacts; d) it is possible to simulate the

considered physical processes in a combined manner (i.e. solving a coupled-field problem) or treat them individually.

Several representative examples of dynamic simulations are provided in the paper, which demonstrate how the PMPG output is influenced by structural and base excitation parameters as well as effect of the surrounding pressure on generated voltage. The model may be successfully used for running various parametric simulations that enable determination and subsequent tuning of device dynamical and electrical performance. The tasks for future work include investigation of the contact-mode operation as well as more thorough investigation of influence of air damping on the operation of the piezotransducer.

Acknowledgment

This research was performed under postdoctoral fellowship, which is funded by EU Structural Funds project "Postdoctoral Fellowship Implementation in Lithuania".

References

[1] Roundy S., **Wright P. K.**, **Rabaey J.**. Energy Scavenging for Wireless Sensor Networks with Special Focus on Vibrations, Kluwer Academic Publishers, 2004.

[2] Vullers R. J. M., van Schaijk R., Doms I., Van Hoof C., Mertens R. Micropower Energy Harvesting, Solid State Electronics, vol. 53, pp. 684-693, 2009.

[3] Cook-Chennault K. A., Thambi N., Sastry A. M. Powering MEMS Portable Devices - a Review of Non-regenerative and Regenerative Power Supply Systems with Special Emphasis on Piezoelectric Energy Harvesting Systems, Smart Materials and Structures, vol. 17, 2008.

[4] Khaligh A., Zeng P., Zheng C. Kinetic Energy Harvesting Using Piezoelectric and Electromagnetic Technologies-State of the Art, IEEE Transactions on Industrial Electronics, vol. 53(3), pp. 850-860, 2010.

[5] Zhu D., Tudor M. J., Beeby S. P. Strategies for Increasing the Operating Frequency Range of Vibration Energy Harvesters: a review, Measurement Science and Technology, vol. 21, 2010.

[6] Ostasevicius V., Milasauskaite I., Dauksevicius R., Baltrusaitis V., Grigaliunas V., Prosycevas I. Experimental Characterization of Material Structure of Piezoelectric PVDF Polymer, Mechanika, vol. 6(86), pp. 78-82, 2010.

[7] Comsol Multiphysics 3.5a software user manual, Piezoelectric Application Modes, 2008.

[8] Yang J. An Introduction to the Theory of Piezoelectricity, Springer Science+Business Media, N.Y., 2005.

[9] Dauksevicius R., Kulvietis G., Ostasevicius V., Milasauskaite I. Finite Element Analysis of Piezoelectric Microgenerator - Towards Optimal Configuration, Process Engineering, vol. 5, pp. 1312-1315, 2010.

[10] Ostasevicius V., Dauksevicius R. Microsystems Dynamics, Springer Science+Business Media, B.V., 2011.

[11] Veijola T., Kuisma H., Lahdenpera J. The Influence of Gas-Surface Interaction on Gas Film Damping in a Silicon Accelerometer, Sensors and Actuators A: Physical, vol. A66, pp. 83-92, 1998.